




## Phononic-magnetic dichotomy of the thermal Hall effect in the Kitaev material $\text{Na}_2\text{Co}_2\text{TeO}_6$

Matthias Gillig <sup>1</sup>, Xiaochen Hong,<sup>1,2</sup> Christoph Wellm,<sup>1</sup> Vladislav Kataev <sup>1</sup>,  
Weiliang Yao,<sup>3</sup> Yuan Li <sup>3,4</sup>, Bernd Büchner,<sup>1,5,6</sup> and Christian Hess <sup>1,6,2,\*</sup>

<sup>1</sup>Leibniz IFW Dresden, Helmholtzstrasse 20, 01069 Dresden, Germany

<sup>2</sup>Fakultät für Mathematik und Naturwissenschaften, Bergische Universität Wuppertal, 42097 Wuppertal, Germany

<sup>3</sup>International Center for Quantum Materials, School of Physics, Peking University, Beijing 100871, China

<sup>4</sup>Collaborative Innovation Center of Quantum Matter, Beijing 100871, China

<sup>5</sup>Institute of Solid State and Materials Physics, TU Dresden, 01069 Dresden, Germany

<sup>6</sup>Center for Transport and Devices, TU Dresden, 01069 Dresden, Germany



(Received 27 March 2023; accepted 19 September 2023; published 3 November 2023)

The quest for a half-quantized thermal Hall effect of a Kitaev system represents an important tool to probe topological edge currents of emergent Majorana fermions. Pertinent experimental findings for  $\alpha\text{-RuCl}_3$  are, however, strongly debated, and it has been argued that the thermal Hall signal stems from phonons or magnons rather than from Majorana fermions. Here, we investigate the thermal Hall effect of the Kitaev candidate material  $\text{Na}_2\text{Co}_2\text{TeO}_6$ , and we show that the measured signal emerges from at least two components, phonons and magnetic excitations. This dichotomy results from our discovery that the longitudinal and transversal heat conductivities share clear phononic signatures, while the transversal signal changes sign upon entering the low-temperature, magnetically ordered phase. Our results demonstrate that uncovering a genuinely quantized magnetic thermal Hall effect in Kitaev topological quantum spin liquids such as  $\alpha\text{-RuCl}_3$  and  $\text{Na}_2\text{Co}_2\text{TeO}_6$  requires disentangling phonon vs magnetic contributions, including potentially fractionalized excitations such as the expected Majorana fermions.

DOI: [10.1103/PhysRevResearch.5.043110](https://doi.org/10.1103/PhysRevResearch.5.043110)

### I. INTRODUCTION

The strongly frustrated Kitaev model describes spin-1/2 degrees of freedom on a honeycomb lattice with bond-dependent interactions [1]. This exactly solvable spin model attracts strong attention in the community because it exhibits a quantum spin liquid (QSL) ground state with peculiar spin excitations which fractionalize into localized  $\mathbb{Z}_2$  gauge fluxes (also called visons) and itinerant Majorana fermions [1–3] which might become exploitable for quantum memories protected from decoherence [1]. Particular interest in this regard has been generated by the expectation that an external magnetic field renders the ground state a topological quantum spin liquid with chiral Majorana edge currents and a field-induced bulk gap. These edge currents are expected to give rise to a thermal Hall signal in experiments [1] with a half-quantized transversal thermal conductivity  $\kappa_{xy}/T$ .

For a few years, the compound  $\alpha\text{-RuCl}_3$  has been considered a prime candidate material [4], for which many experimental probes hint at compatibility with the characteristics of Kitaev's model [5]. Indeed, this compound exhibits a sizable thermal Hall effect [6–11]. Interestingly, for certain

ranges of temperature and magnetic field, a plateau has been reported in  $\kappa_{xy}/T$  at a value which corresponds to exactly 1/2 of the quantum of the two-dimensional thermal Hall conductance  $K_{QH}/T = \frac{\pi^2 k_B^2}{3h}$  [7,9,11,12], a result which could be recognized as the key fingerprint of the topologically protected Majorana edge currents. However, there are concerns about the uniqueness of this finding, and topological magnons [13] as well as chiral phonons [8,10] have been suggested as alternative origins of the thermal Hall effect in  $\alpha\text{-RuCl}_3$ .

Recently,  $\text{Na}_2\text{Co}_2\text{TeO}_6$  was proposed as a novel possible materialization of Kitaev physics in a honeycomb lattice [14,15], originating from the expectation of a bond-dependent Ising-like interaction between the pseudospin-1/2 of the  $d^7 \text{Co}^{2+}$  ions in the high-spin  $t_{2g}^5 e_g^2$  configuration [14,16]. The material orders antiferromagnetically below  $T_N \approx 27 \text{ K}$ , and zigzag [17] and triple- $\mathbf{q}$  [18–20] ground states were proposed following neutron scattering data. The magnetically ordered ground state implies the significance of Heisenberg and/or off-diagonal interactions in addition to the expected primary Kitaev coupling [21,22]. An in-plane magnetic field was found to suppress the magnetic order at  $\mu_0 H > \mu_0 H_c \approx 10 \text{ T}$ , in favor of strong low-energy spin fluctuations at fields near  $H_c$  which are compatible with a field-induced QSL [23]. Altogether, these features bear an astonishing similarity to the magnetic phase diagram of  $\alpha\text{-RuCl}_3$  [23].

Here, we present the thermal Hall effect results of  $\text{Na}_2\text{Co}_2\text{TeO}_6$  which have been registered in both the magnetically ordered and paramagnetic phases, where the latter in particular can be expected to host quantum spin fluctuations which emerge from the extended Kitaev-Heisenberg

\*c.hess@uni-wuppertal.de

Published by the American Physical Society under the terms of the [Creative Commons Attribution 4.0 International](https://creativecommons.org/licenses/by/4.0/) license. Further distribution of this work must maintain attribution to the author(s) and the published article's title, journal citation, and DOI.

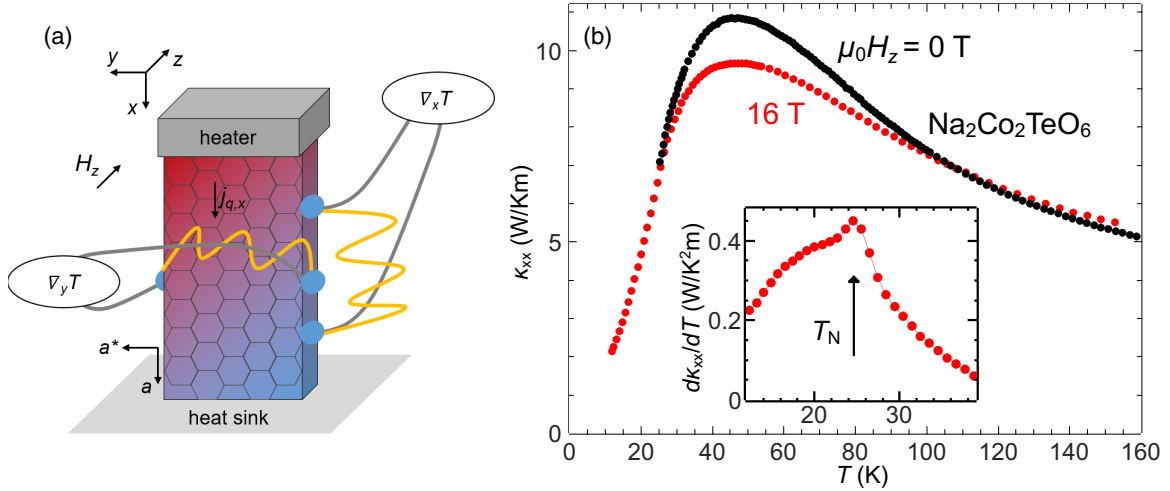


FIG. 1. Experimental setup scheme and longitudinal heat conductivity data for  $\text{Na}_2\text{Co}_2\text{TeO}_6$ . (a) Experimental setup indicating the orientations of the thermal current density  $j_{q,x}$  and the longitudinal temperature gradient  $\nabla_x T$  parallel to the  $a$  axis of the compound and the magnetic field  $H_z$  along the  $c$  axis (perpendicular to the planes). The transverse temperature gradient  $\nabla_y T$  is measured perpendicular to the thermal current and the magnetic field. This corresponds to a standard Hall configuration. Yellow lines represent the Au/Fe thermocouples. (b) Temperature dependence of the longitudinal heat conductivity  $\kappa_{xx}$  of  $\text{Na}_2\text{Co}_2\text{TeO}_6$  at zero field and at magnetic field  $\mu_0 H_z = 16$  T. The inset shows the temperature derivative  $d\kappa_{xx}/dT$  of the longitudinal thermal conductivity at 16 T.

spin model considered for this compound. The transverse thermal conductivity  $\kappa_{xy}$  is sizable in the whole regime of temperature and magnetic field studied and similar to those recently reported in pioneering studies of  $\kappa_{xy}$  [24,25]. In this work we discover that, interestingly, the temperature and magnetic field dependences of  $\kappa_{xy}$  possess a tight connection to those of the essentially phononic longitudinal thermal conductivity  $\kappa_{xx}$  [23]. This clearly suggests that also  $\kappa_{xy}$  arises by a considerable amount due to phononic heat conduction. However, despite the global sign change of  $\kappa_{xy}$  deep in the magnetically ordered phase, specific field induced anomalies in both  $\kappa_{xx}$  and  $\kappa_{xy}$  do not undergo a sign change. By means of electron spin resonance (ESR) we unambiguously relate these anomalies to the impact of resonant magnon-spin scattering on phononic transport. Thus, we argue that the thermal conductivity  $\kappa_{xy}$  consists of a phononic contribution and at least one other contribution of a different, presumably magnetic, origin of opposite sign.

## II. EXPERIMENT

High-quality  $\text{Na}_2\text{Co}_2\text{TeO}_6$  single crystals were grown by a modified flux method [15,26]. A regular bar-shaped sample of  $5.05 \times 1.03 \times 0.10 \text{ mm}^3$  was cut from an as-grown crystal with the sample edges parallel to the  $a$ ,  $a^*$ , and  $c$  axes, respectively. The cut sample was directly mounted onto a large metallic heat sink in a home-built probe, employing a six-point measurement geometry [see Fig. 1(a)]. In our configuration, a thermal current density  $j_{q,x} = P/A$  (with heater power  $P$  and sample cross-sectional area  $A$ ) was generated parallel to the  $a$  axis (i.e., the zigzag direction of the honeycomb lattice) using a chip heater ( $R = 2.7 \text{ k}\Omega$ ). The thereby produced longitudinal thermal gradient  $\nabla_x T = \Delta_x T/d$  was determined by measuring the temperature difference  $\Delta_x T$  between the contacts of a field-calibrated differential Au/Fe-chromel thermocouple at distance  $d$ . The

transverse temperature gradient  $\nabla_y T = \Delta_y T/w$  along the  $a^*$  direction which arises upon applying a magnetic field parallel to the  $c$  axis, i.e., perpendicular to the honeycomb layers, was measured by a second thermocouple of the same type.  $w$  is the distance of the transverse thermocouple contacts along the sample width. The thermocouples were fabricated from Au-0.07 at. % Fe and chromel wire pairs. A wire cross section of  $76 \mu\text{m}$  and extended wire lengths of 4 and 8 cm for the chromel wire and the Au/Fe wire, respectively, guarantee negligible heat loss through the thermocouples.

For the field calibration of the thermocouples, the thermocouples were first mounted on a piece of fused silica. Afterwards, the thermocouple voltage generated by a temperature gradient on the fused silica piece was isothermally measured while slowly ramping the magnetic field. This procedure was performed for a suitable set of temperatures in order to cover the field and temperature range explored in our experiment.

The longitudinal  $\nabla_x T$  and the transversal  $\nabla_y T$  were measured simultaneously. The small size of the transverse signal required the application of a large heat current to achieve a reasonable signal-to-noise ratio, resulting in temperature differences on the order of  $\Delta_x T/T_0 = 10\%$  and  $\Delta_y T/T_0 = 0.01\%$  compared to the thermal bath temperature  $T_0$ . At fixed temperature, the transverse gradient  $\nabla_y T$  was verified to linearly depend on the heater power. Therefore, unwanted effects which might occur due to the relatively large heater power are excluded. To consider the elevated temperature at the transverse thermocouple position due to the sizable temperature gradient we estimated this temperature by extrapolating  $T_0$  to the position of the transverse thermocouple in the center of the sample. To eliminate longitudinal contributions to the transverse signal due to a possible misalignment of the thermocouple contacts, measurements were performed under both field polarities, and longitudinal components were eliminated by antisymmetrization of  $\nabla_y T$ . Eventually, using Fourier's

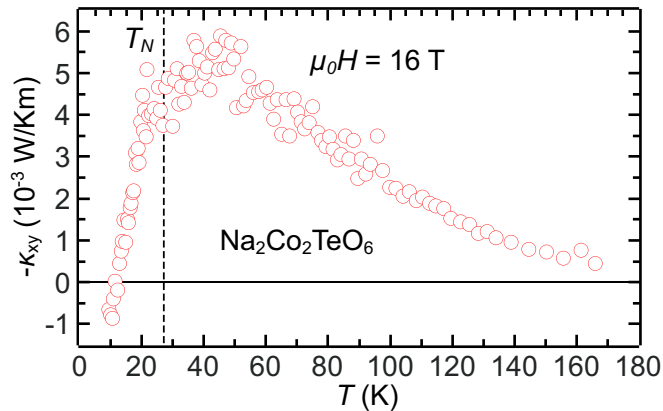


FIG. 2. Temperature dependence of the transverse heat conductivity  $\kappa_{xy}$  of  $\text{Na}_2\text{Co}_2\text{TeO}_6$  with the heat current  $j_{q,x}$  along the  $a$  axis at zero field and at a magnetic field  $\mu_0 H_z = 16$  T along the  $c$  axis.

law the longitudinal thermal conductivity was calculated as  $\kappa_{xx} = j_{q,x}/|\nabla_x T|$ , and the transverse thermal conductivity was yielded by  $\kappa_{xy} = \kappa_{xx}^2 \nabla_y T / j_{q,x}$ . For the latter, we approximate  $\kappa_{xx} \approx \kappa_{yy}$ , which holds modulo a small anisotropy of the order of unity [23].

High-field, high-frequency electron spin resonance (HF-ESR) experiments were carried out in the frequency range 250–950 GHz using a home-made multifrequency spectrometer. For the generation and detection of the microwave radiation a vector network analyzer (PNA-X from Keysight Technologies) and a combination of a modular amplifier/multiplier chain (Virginia Diodes, Inc.) and a hot electron InSb bolometer (QMC Instruments) were employed. A single crystal of  $\text{Na}_2\text{Co}_2\text{TeO}_6$  was mounted in a probe head operational in the transmission mode that was put in a  $^4\text{He}$  variable-temperature insert of a superconducting magnet system (Oxford Instruments) producing fields up to 16 T (see also Refs. [27–29]).

### III. RESULTS

#### A. Temperature dependence of $\kappa_{xx}$ and $\kappa_{xy}$

Figure 1(b) shows a comparison of  $\kappa_{xx}$  at zero magnetic field, which is very similar to our previous findings [23], and at  $\mu_0 H = 16$  T with  $\mathbf{H} \parallel c$ . Apparently, apart from a slight reduction of about 11%, the overall curve shape is preserved even at this relatively large field. Only a weak change is observed in the onset temperature of magnetic ordering, which we infer from the cusp in  $d\kappa_{xx}/dT$  shown in the inset of Fig. 1(b) as  $T_N \approx 25$  K, which is only slightly lower than in zero field [15,23]. Note that an in-plane magnetic field was reported to have a much stronger impact:  $\kappa_{xx}$  becomes strongly enhanced, while the magnetic order is suppressed for  $\mu_0 H \gtrsim 10$  T [23].

Figure 2 presents our findings for the transversal heat conductivity  $\kappa_{xy}$  at 16 T as a function of temperature. At first glance, one can recognize strong similarities between  $\kappa_{xx}$  and  $-\kappa_{xy}$  (as plotted). Both curves rapidly rise with increasing temperature  $T$ , exhibit a broad peak at about 40–50 K, and then gradually decay to lower values with further rising  $T$ . However, different from the longitudinal thermal conductivity,

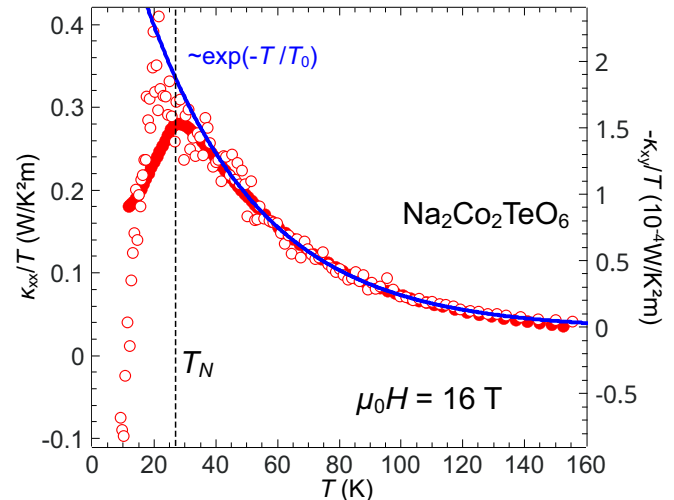


FIG. 3. Comparison of  $-\kappa_{xy}/T$  (open circles, right scale) and  $\kappa_{xx}/T$  (solid circles, left scale) for  $\text{Na}_2\text{Co}_2\text{TeO}_6$  at  $\mu_0 H = 16$  T directed along the  $c$  axis. The solid line shows a fit according to  $\kappa_{xy}/T = A \exp(-T/T_0) + B$  [30] for  $T > 35$  K with the parameters  $A = -3.93 \times 10^{-4}$  W/K<sup>2</sup> m,  $B = 2.06 \times 10^6$  W/K<sup>2</sup> m, and  $T_0 = 36.8$  K.

which can have only positive values,  $\kappa_{xy}$  changes sign from positive values at  $T \lesssim 12$  K to negative values at higher  $T$ .

In order to disentangle the possible origins of the observed thermal Hall effect (magnetic or phononic), we further investigate in Fig. 3 the temperature dependence of  $-\kappa_{xy}/T$ . Remarkably, in this representation, a strong cusplike anomaly is present close to the magnetic ordering temperature  $T_N$ , which separates a region  $T \lesssim T_N$  with a very steep temperature dependence, including the sign change from the high-temperature region  $T \gtrsim T_N$ , where  $\kappa_{xy}/T$  decays moderately with rising temperature.

We first focus on the latter paramagnetic regime. Here, the transversal heat conductivity follows very well an exponential scaling  $\kappa_{xy}/T \sim \exp(-T/T_0)$  which recently was proposed as a generic feature for the temperature dependence of the thermal Hall effect of charge-neutral excitations [30]. According to the modeling, the observation of this scaling suggests a nontrivial topology of the heat carrying quasiparticles with a finite and essentially temperature-independent effective Berry curvature density. Unfortunately, the exponential scaling is expected to universally hold for all types of quasiparticles, and thus, it does not allow us to draw clear-cut conclusions about the type of excitation causing the thermal Hall effect. However, a direct comparison of  $-\kappa_{xy}/T$  with  $\kappa_{xx}/T$  (see Fig. 3) strikingly yields a perfect match of both curves for  $T > T_N$ , i.e., in the whole paramagnetic regime. The only difference is a temperature-independent offset since  $\kappa_{xy}/T \rightarrow 0$  at high temperature, whereas  $\kappa_{xx}/T$  approaches a finite value. Thus, in view of the almost perfect matching temperature dependences of  $\kappa_{xx}/T$  and  $\kappa_{xy}/T$  and the fact that the heat carrying quasiparticles contributing to the longitudinal  $\kappa_{xx}$  are phonons (see Ref. [23] and further discussion below), it is tempting to interpret this observation as evidence of a phononic origin of the thermal Hall for  $T \gtrsim T_N$ . Indeed, this conclusion seems to be corroborated by findings for  $\alpha\text{-RuCl}_3$  in which the

similarities between  $\kappa_{xx}/T$  and  $\kappa_{xy}/T$  have been interpreted as significant evidence of a phononic origin of the thermal Hall effect [10]. Furthermore, the recent demonstrations of the phonon thermal Hall effect in several magnetic insulators supports the notion that similar temperature dependences of  $\kappa_{xy}/T$  and a phononic  $\kappa_{xx}/T$  are a general fingerprint of the phononic thermal Hall effect [31–33].

However, the low- $T$  behavior of  $\kappa_{xy}$  in the magnetically ordered regime is difficult to explain by a sole phononic contribution to  $\kappa_{xy}$ . As can be inferred clearly from the data in Fig. 3,  $\kappa_{xx}/T$  and  $\kappa_{xy}/T$  exhibit distinctly different temperature dependences at  $T \lesssim T_N$ . While upon cooling  $\kappa_{xx}/T$  is only moderately reduced by about 30% at the lowest temperature measured,  $-\kappa_{xy}/T$  decreases much more steeply and changes sign at about 12 K. This sign change is crucial information which implies either of two scenarios for the origin of the thermal Hall effect.

It is conceivable, on the one hand, that  $\kappa_{xy}$  indeed is purely phononic, as inferred above. If this were the case, the mechanism causing the off-diagonal thermal response would have to fundamentally change upon cooling through  $T_N$  and further upon possible reorientations of the magnetic order [23] at even lower temperatures. Given the rather complicated and barely understood magnetic phase diagram of  $\text{Na}_2\text{Co}_2\text{TeO}_6$  [15,23,34,35], one cannot straightforwardly exclude this possibility without further information. One should note, however, that up to now, no reported examples of the phonon thermal Hall effect exhibit a sign change [31–33,36–42]. Hence, this scenario seems rather unlikely [43].

On the other hand, if one assumes that the sign of the phonon thermal Hall in  $\text{Na}_2\text{Co}_2\text{TeO}_6$  effect is always *negative*, the only possibility is that a second *positive* contribution to  $\kappa_{xy}$  rapidly gains importance, causing the sign change of  $\kappa_{xy}$  in the magnetically ordered phase. In this case, this second contribution must be due to transport by magnetic degrees of freedom. Among these, within this paper we do not distinguish further since magnetic fluctuations remain strong even at low temperature [23], and hence, both magnons and possible fractionalized excitations such as Majorana fermions and visons *a priori* cannot be excluded.

### B. Magnetic field dependence of $\kappa_{xx}$ and $\kappa_{xy}$

The latter scenario of a two-component thermal Hall conductivity is strongly supported by the isothermal magnetic field dependence of  $\kappa_{xy}$  as presented in Fig. 4(a) at selected temperatures of 8, 16, and 37 K. As can be clearly inferred from the data,  $\kappa_{xy}(H)$  at all these temperatures exhibits a pronounced and mostly nonmonotonic field dependence. This is at odds with the magnetization, which increases monotonically with field [35]. The nonmonotonic field dependence is also unusual since it is in strong contrast to other findings on various nonferromagnetic materials, including  $\alpha\text{-RuCl}_3$ , in which a quasilinear field dependence of  $\kappa_{xy}(H)$  and a concomitant monotonic magnetization have been observed [6,8,36,39–41,44].

The origin of the unusual  $\kappa_{xy}(H)$  can straightforwardly be connected to the field dependence of the isothermally measured  $\kappa_{xx}(H)$ , as shown in Figs. 4(b)–4(d), which we will

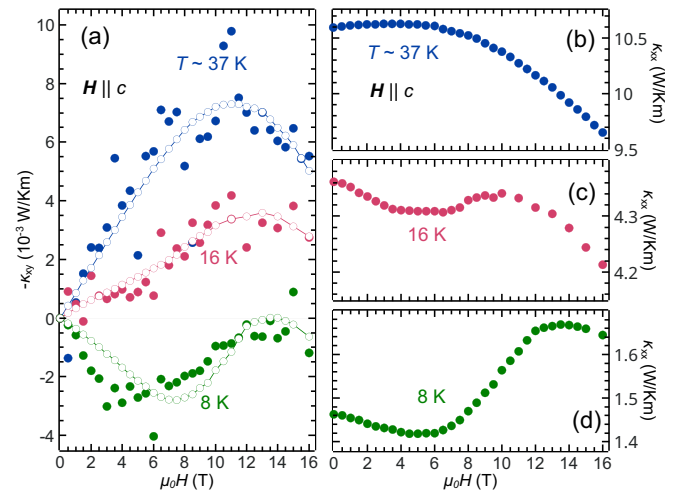


FIG. 4. Field dependence of the longitudinal and transversal thermal conductivities of  $\text{Na}_2\text{Co}_2\text{TeO}_6$  for selected temperatures. (a) Field dependence of the transverse thermal conductivity  $\kappa_{xy}$ . Open circles represent a fit according to Eq. (2) using  $\kappa_{xx}$  data. [(b)–(d)] Field dependence of the longitudinal thermal conductivity  $\kappa_{xx}$ .

discuss in detail further below.  $\kappa_{xx}(H)$  possesses two features with opposite trends in temperature. One is a pronounced minimum at about 4–8 T which is strongest at 8 K, very weak at 16 K, and absent at 37 K. The other is a decrease at higher field with increasing field. At 8 K the decrease is weak and discernible only for  $\mu_0 H > 14$  T, but with rising temperature it becomes increasingly important. At 16 K it begins at around 10 T, and at 37 K it dominates the data for  $\mu_0 H \gtrsim 4$  T. Clearly, the growing importance is consistent with the data shown in Fig. 1(b).

These  $\kappa_{xx}(H)$  data are characteristic of a phonon heat conductivity which is subject to strong phonon-spin scattering [45–48]. In fact,  $\kappa_{xx}$  has already been shown to be governed by phonons with strong phonon-spin scattering for magnetic fields applied in plane [23]. In the situation which we consider here, i.e., with a magnetic field perpendicular to the magnetic planes, for the  $(H, T)$  dependence of  $\kappa_{xx}$  one should consider two qualitative phonon-spin scattering mechanisms: In the magnetically ordered state  $T \leq T_N$  one can expect the phonon spin scattering to become particularly important (i) near field-driven spin reorientation transitions [48] and (ii) due to “resonant” scattering of the phonons off collective excitations such as magnons [23,46,47].

Concerning the former, an initial version of the magnetic  $(H, T)$ -phase diagram for  $H||c$  [35] revealed a practically temperature independent magnetic transition at about 8 T for  $T \lesssim 16$  K. Associated spin fluctuations are therefore a plausible cause for the dip observed in  $\kappa_{xx}(H)$  at 8 and 16 K.

On the other hand, clear-cut information about low-energy magnon excitations in zero field is available from recent inelastic neutron scattering (INS) data [49]. The lowest-lying magnon mode has been reported in the energy range of 1–3 meV with minima at the  $\Gamma$  and  $M$  points. It is thus clear, if one considers a typical  $\Theta_D$  of a few hundred kelvin, that phonon-magnon scattering involving the acoustic phonon modes must be significant already at zero field. In order to



obtain further insight in the field and temperature dependence of the magnon mode and  $\kappa_{xx}(H)$ , we investigated the magnetic field induced energy shift of this magnon mode at the  $\Gamma$  point by means of HF-ESR (see Appendix A). At  $T = 3$  K, the data yield an energy gap at the  $\Gamma$  point of about 219 GHz (0.91 meV) at zero field, in accordance with the zero-field neutron result, and a Zeeman shift to about 950 GHz (about 3.9 meV) at 14 T (corresponding to a  $g$  factor of 3.91).

If one assumes a rigid magnon band shift in magnetic field, the maximum magnon energy at 16 T amounts to about 6.8 meV, corresponding to about 80 K. Standard considerations for phonon heat conductivity [50,51], namely,

$$\kappa_{\text{ph}} \propto T^3 \int_0^{\Theta_D/T} \frac{x^4 \exp(x)}{[\exp(x) - 1]^2} \tau_c dx, \quad (1)$$

with  $\tau_c$  being a total phononic relaxation time, imply phonons with an energy of about  $4k_B T$  dominate the heat conductivity. Thus, within a simple kinematic picture for the phonon-magnon scattering, for temperatures smaller than some characteristic  $T_{\text{peak}} < (80 \text{ K}/4) \lesssim 20$  K one would naturally expect a minimum in  $\kappa_{xx}(H)$  because in this  $T$  range the magnetic field should drive the “intersection” of the phonon and magnon bands through the peak of the integrand in Eq. (1). At higher temperatures, the applied magnetic field is sufficient only to drive the band intersection *towards* the integrand peak without actually reaching it, and therefore, the data should exhibit only suppression with increasing field. Both the minimum at low  $T$  and the increasing high-field suppression are qualitatively observed, superimposed on the effect of the phase transition described above.

The above considerations should be understood within some margin of error: The actual  $T_{\text{peak}}$  and further details of  $\kappa_{xx}(H, T)$  certainly depend on the true  $\Theta_D$ , the magnon density of states, and the effects of temperature and magnetic field on the magnon dispersion. Concerning the latter, it is worth pointing out that our ESR data imply that at  $T = 6\text{--}8$  K the magnon mode starts to increasingly soften and broaden with increasing temperature, consistent with the zero magnetic field results of INS [49]. The broadening gets particularly strong at  $T > 20$  K, still below  $T_N$ , possibly due to enhancement of the spin fluctuations when approaching the phase transition. It is plausible that for  $T > T_N$  a qualitatively similar scenario applies for paramagnon excitations.

After establishing the phonon-only nature of  $\kappa_{xx}(H)$  and the connection of its anomalous field dependence to phonon-magnon scattering, we turn now to  $\kappa_{xy}(H)$  and directly compare the data for the longitudinal and transverse heat transport channels. Very clearly, at 8 K both curves for  $\kappa_{xx}(H)$  and  $-\kappa_{xy}(H)$  possess a very similar relative field dependence, i.e., a minimum at 4–6 T and a saturation at  $\mu_0 H \gtrsim 12$  T. At the higher temperatures, 16 and 37 K, the connection between  $\kappa_{xx}(H)$  and  $-\kappa_{xy}(H)$  at first glance does not seem as clear as that for 8 K. However, closer inspection reveals that for all data the derivative  $\partial\kappa_{xy}(H)/\partial H$  is proportional to  $\kappa_{xx}(H)$  modulo a constant offset. In order to demonstrate this revealing connection we plot in Fig. 4(a) a fit

according to

$$\kappa_{xy}(H) = a_1 \kappa_{xx}(H) \mu_0 H + a_2 \mu_0 H, \quad (2)$$

with  $a_1$  and  $a_2$  being fitting constants [52]. As can be seen in the figure, this empirical ansatz describes the data very well, apart from a slight low-field deviation at 8 K, yielding parameters  $a_1 < 0$  and  $a_2 > 0$  (see Appendix B).

Equation (2) clearly suggests that  $\kappa_{xy}$  is composed of two additive components with opposite signs. Due to its weighting with the phononic  $\kappa_{xx}$ , the first term can be assigned to a phononic thermal Hall effect  $\kappa_{xy,\text{ph}}$ . On the other hand, the second term is strictly linear in magnetic field, which corresponds to lowest order to the usual observation for  $\kappa_{xy}(H)$  for the vast majority of compounds (see above). This component must have a different origin than  $\kappa_{xy,\text{ph}}$ . The most straightforward conclusion is thus that this positive component is magnetic in nature ( $\kappa_{xy,\text{mag}}$ ). Thus, the measured total thermal Hall effect should be understood as the sum of the phononic and magnetic contributions to the thermal Hall effect, i.e.,  $\kappa_{xy} = \kappa_{xy,\text{ph}} + \kappa_{xy,\text{mag}}$ . The observed sign change in the measured  $\kappa_{xy}$  indicates a change in the dominance of one component with respect to the other.

Qualitatively, within a semiclassical picture, the direct proportionality of  $\kappa_{xy,\text{ph}}(H)$  to  $\kappa_{xx}(H)$  implies that the phononic transverse transport channel possesses an unusual direct linear dependence of the field-dependent phonon relaxation time  $\tau_c(H)$ . Future models of the phononic thermal Hall effect therefore should accommodate for this observation.

It is instructive to extract the separate temperature dependences of  $\kappa_{xy,\text{ph}}$  and  $\kappa_{xy,\text{mag}}$ , which straightforwardly can be achieved for selected temperatures from the fits shown in Fig. 4. In addition, we use two temperature-dependent data sets for  $\kappa_{xx}$  and  $\kappa_{xy}$  measured at  $\mu_0 H = 6$  and 16 T (see Appendix B) and Eq. (2) to extract  $\kappa_{xy,\text{ph}}$  and  $\kappa_{xy,\text{mag}}$  at 16 T. The complete data set is shown in Fig. 5 in comparison with the total measured  $\kappa_{xy}$  as a function of temperature. This comparison clearly reveals that for  $T > T_N$  the absolute value of  $\kappa_{xy,\text{ph}}$  is always somewhat larger than that of  $\kappa_{xy,\text{mag}}$ , yielding the overall negative sign. However, upon the onset at  $T < T_N$ , this fine balance changes, and  $\kappa_{xy,\text{mag}}$  exceeds  $|\kappa_{xy,\text{ph}}|$ , leading to the sign change of  $\kappa_{xy}$  at low temperature. The importance of the onset of magnetic order can also be inferred from the temperature dependence of parameters  $a_1$  and  $a_2$ . While both follow a very similar temperature dependence for  $T > T_N$ , they become off balance at  $T < T_N$  (see Fig. 11 in Appendix B).

A quantitative consistency check of our analysis can be obtained from the thermal Hall angle. Interestingly, if one considers the total measured Hall angle of  $\text{Na}_2\text{Co}_2\text{TeO}_6$ , it is of the order of  $5 \times 10^{-4}$  close to  $T_N$  and decays further with increasing temperature [see Fig. 12(a) in Appendix B]. This value is significantly smaller than that of all other reported insulators [41]. This can be more clearly seen by considering the length scale  $\Lambda_{\text{tha}} = l_B \sqrt{\kappa_{xy}/\kappa_{xx}}$ , with  $l_B^2 = \hbar/eB$ . Recently, this quantity was investigated in a comparative analysis of the thermal Hall angle of various insulating compounds with a putative phononic thermal Hall effect [41]. More specifically, it was observed that  $\Lambda_{\text{tha}}$  is within the margin of 2–7 Å, and a quantitative plausibility criterion for a phononic thermal Hall effect is that  $\Lambda_{\text{tha}}$  has a magnitude similar to the shortest

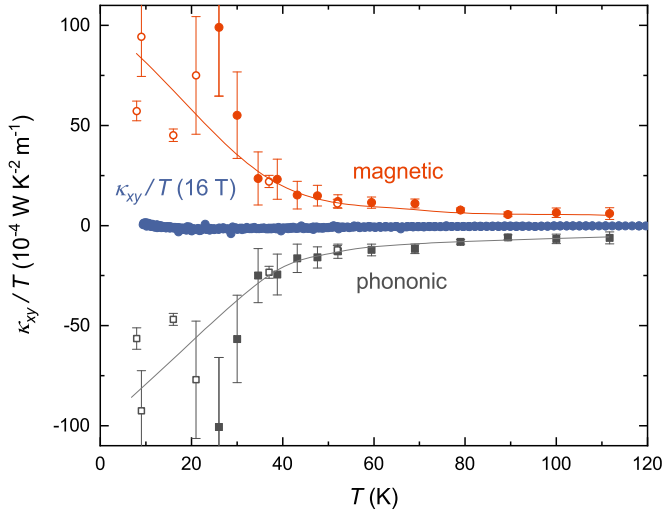


FIG. 5. Decomposition of  $\kappa_{xy}/T$  for  $\text{Na}_2\text{Co}_2\text{TeO}_6$  at 16 T in a negative phononic contribution and a positive magnetic contribution according to fitting results of Eq. (2) compared to the experimental data (blue). Open symbols refer to fits of the field dependence, whereas solid symbols represent fits to data of temperature-dependent measurements. Error bars represent the uncertainty of the fit results. Solid lines are guides to the eye.

possible acoustic phononic wavelength, i.e., the lattice constant. For  $\text{Na}_2\text{Co}_2\text{TeO}_6$ , we find  $\Lambda_{\text{tha}} \sim 1.5 \text{ \AA}$  or lower [Fig. 12(b)], which is much smaller than the lattice constant and clearly is outside of the reported margin of  $\Lambda_{\text{tha}}$ . On the other hand, for the phononic part of the thermal Hall effect  $\kappa_{xy,\text{ph}}$  we find  $\Lambda_{\text{tha}} \sim 6 \text{ \AA}$  [see Fig. 12(c)], which is very compatible with the lattice constant  $a \approx 5.3 \text{ \AA}$  [26] and is well within the above-mentioned margin for  $\Lambda_{\text{tha}}$ . Thus, our analysis is independently quantitatively corroborated, and the

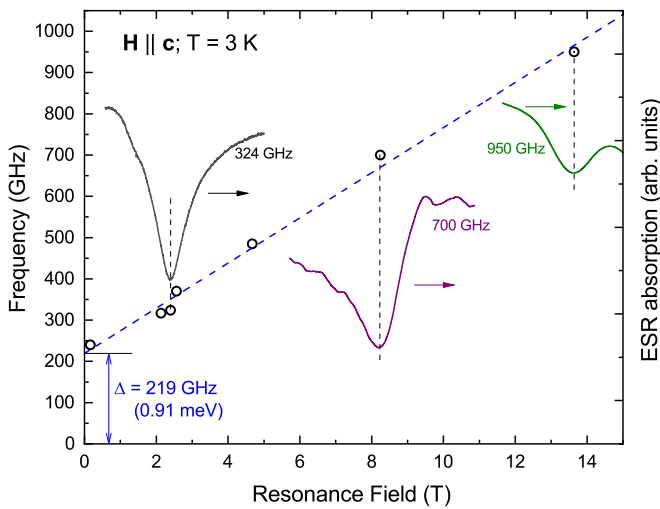


FIG. 6. Frequency  $\nu$  versus the resonance field  $H_{\text{res}}$  dependence of the ESR signal of  $\text{Na}_2\text{Co}_2\text{TeO}_6$  for the  $\mathbf{H} \parallel c$  axis field geometry at  $T = 3 \text{ K}$  (left vertical scale) together with representative HF-ESR spectra at selected frequencies (right vertical scale). The dashed line depicts the linear dependence  $\nu = \Delta + h^{-1} g_c \mu_0 \mu_B H$ , with a  $g$  factor  $g_c = 3.91$  and a zero-field magnon gap  $\Delta = 219 \text{ GHz}$  ( $0.91 \text{ meV}$ ).

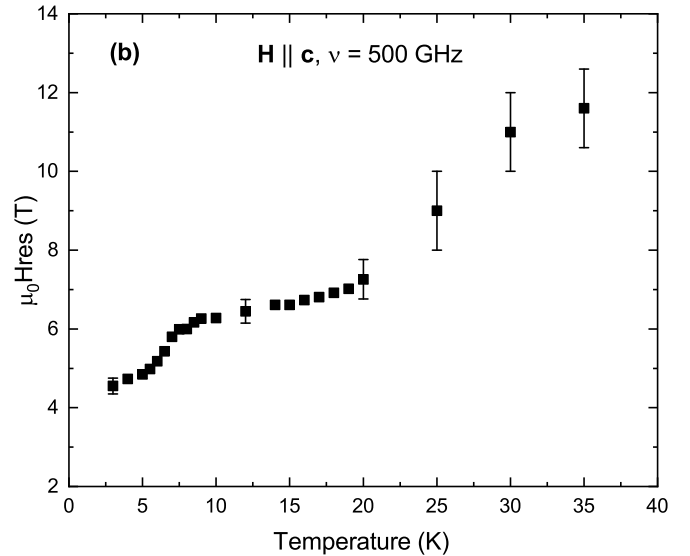
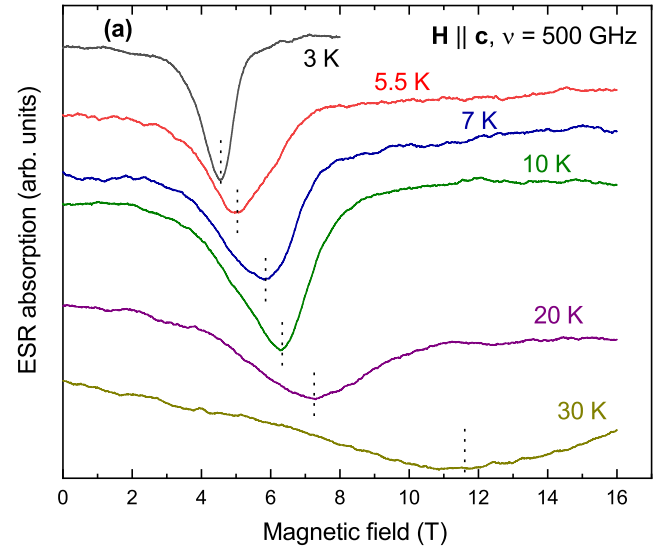


FIG. 7. Temperature dependence of (a) the ESR spectrum at  $\nu = 500 \text{ GHz}$  for  $\mathbf{H} \parallel c$  axis and (b) the resonance field  $H_{\text{res}}$  of the ESR line.

unusual small thermal Hall angle in  $\text{Na}_2\text{Co}_2\text{TeO}_6$  is reconciled by the separation of  $\kappa_{xy}$  into the phononic and magnetic parts.

#### IV. DISCUSSION AND SUMMARY

Our finding of a two-component thermal Hall effect, i.e., with phononic and magnetic contributions, should be placed into the context of recent theoretical and experimental findings. First of all, our conclusion of a sizable  $\kappa_{xy,\text{ph}}$  is very compatible with several recent theoretical works for magnetic systems [53–56] in which phonon-spin scattering was identified as one important source for generating finite phononic transverse thermal conductivity. Indeed, as demonstrated above, phonon-spin scattering is the primary scattering process in the phononic  $\kappa_{xx}$  at all temperatures considered. Other mechanisms for generating a sizable phononic thermal Hall effect, in particular scattering off charged impurities [57], are thus less important in  $\text{Na}_2\text{Co}_2\text{TeO}_6$ . On the other hand, a mag-

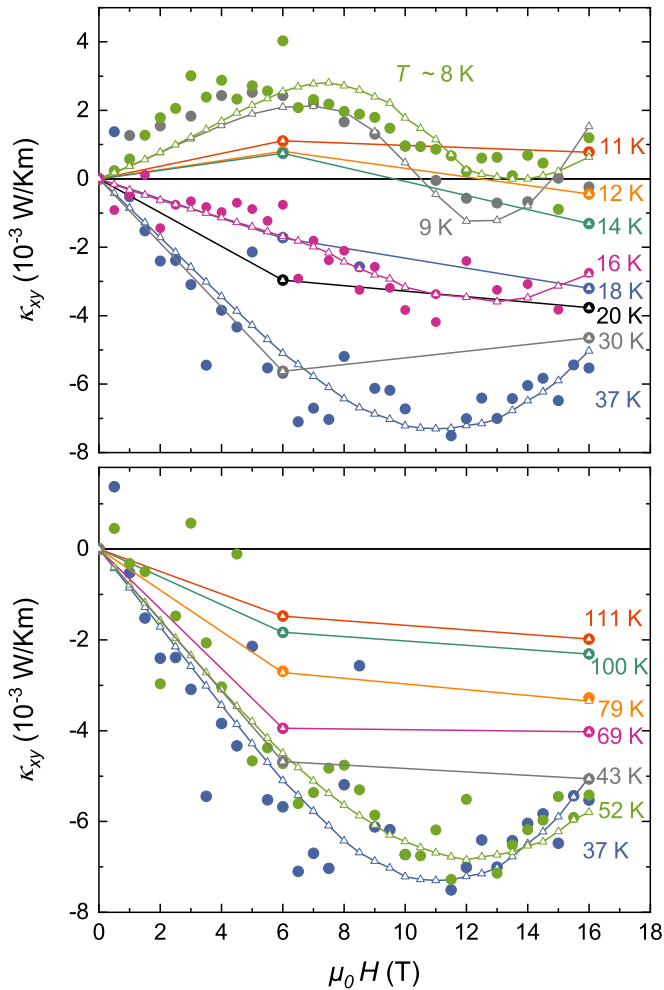


FIG. 8. Field dependence of the thermal Hall effect of  $\text{Na}_2\text{Co}_2\text{TeO}_6$  for selected temperatures where filled symbols represent experimental data and open triangles stand for fits according to Eq. (2) using xx-data. Solid lines are guides to the eye.

netic thermal Hall effect has been shown to be expected for chiral magnons in Kitaev magnets [58], in addition to the expectation of a thermal Hall effect from Majorana fermion edge currents [1,59]. The growing importance of  $\kappa_{xy,\text{mag}}$  observed at  $T < T_N$  in our data seems, indeed, to be compatible with an additional effect due to chiral magnons. For  $T > T_N$ , the chiral magnons are absent, but paramagnonlike fluctuations can be expected and are also detectable by ESR. Here, we conjecture that the decay of the transverse signal is related to the thermal decay of spin correlations. Intriguingly, in this regime, the data suggest that  $\kappa_{xy,\text{mag}}$  and  $\kappa_{xy,\text{ph}}$  have similar magnitudes and temperature dependence, yielding an almost compensated total thermal Hall effect. This observation, which deserves further investigation, might be key for unraveling the underlying physics. We point out that a microscopic mechanism, as well as a quantitative and qualitative prediction of the phononic and magnetic thermal Hall effect in  $\text{Na}_2\text{Co}_2\text{TeO}_6$  and, more generally, in Kitaev systems, still needs to be worked out. Also, a finite magnetic thermal Hall effect is very compatible with the apparent absence of a magnetic contribution to  $\kappa_{xx}$  since  $\kappa_{xy}$  is expected to be independent of the magnon lifetime

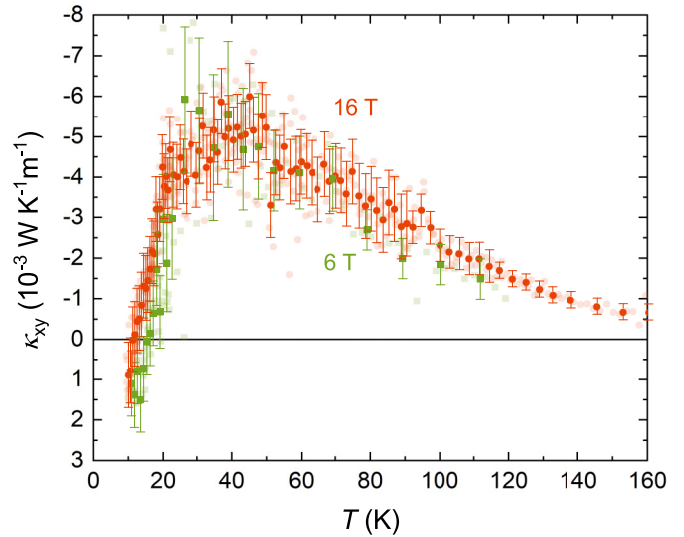


FIG. 9. Temperature dependence of the thermal Hall effect of  $\text{Na}_2\text{Co}_2\text{TeO}_6$  for magnetic field applied along the c-axis. Bold symbols represent the four-point average of the data (transparent symbols) and error bars account the spread before averaging.

$\tau$ , in contrast to  $\kappa_{xx}$ , which is linear in  $\tau$  [60]. A very short  $\tau$  should naturally be expected in view of the strong fluctuating nature of magnetism in  $\text{Na}_2\text{Co}_2\text{TeO}_6$  and explains the negligible importance of magnetic  $\kappa_{xx}$ .

In a general scheme, our results also provide fresh input for understanding the controversially discussed thermal Hall effect in  $\alpha\text{-RuCl}_3$ . The experimental significance of a phononic thermal Hall effect as shown in our data for  $\text{Na}_2\text{Co}_2\text{TeO}_6$  implies that a sizable phononic thermal Hall effect should be expected in  $\alpha\text{-RuCl}_3$ , too, because the two systems have a very similar phonon-spin scattering phenomenology [23,46]. Therefore, our results support the recent notion of a phononic thermal Hall effect in  $\alpha\text{-RuCl}_3$  [10] and call for reinvestigation of the intriguing findings for a low-temperature plateau

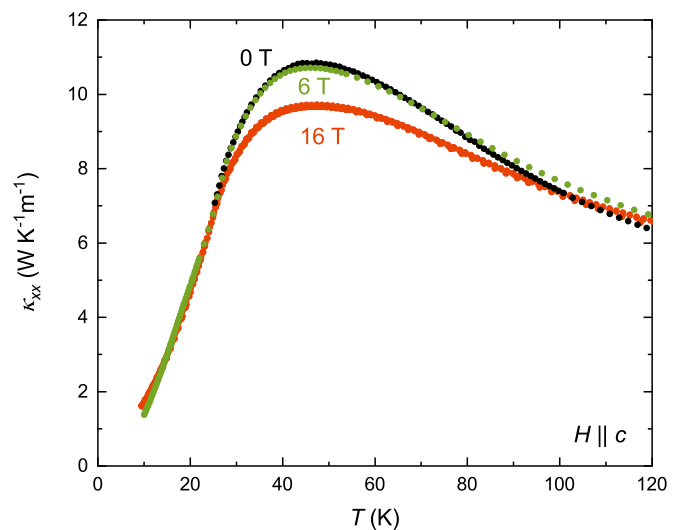


FIG. 10. Temperature dependence of the thermal conductivity of  $\text{Na}_2\text{Co}_2\text{TeO}_6$  for magnetic field applied along the c-axis.

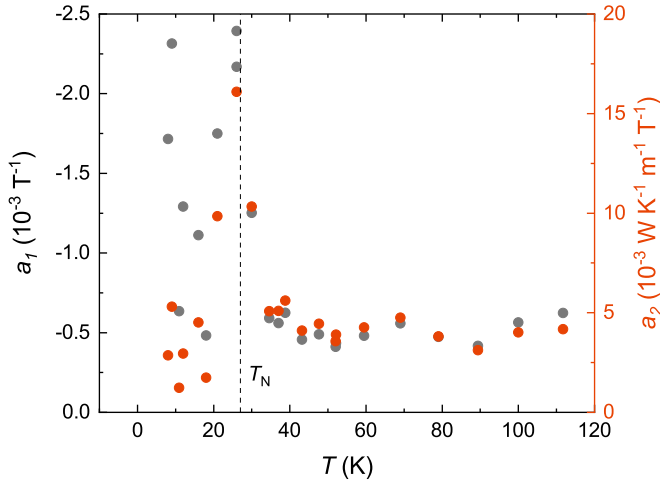


FIG. 11. Temperature dependence of the fit parameters in Eq. (2) (see also Table I).

[7,11]. More specifically, the key for uncovering a genuinely quantized magnetic thermal Hall effect should be to disentangle phonon vs magnetic contributions to  $\kappa_{xy}$  and to look for quantized behavior only in the magnetic part, rather than in the total  $\kappa_{xy}$ , which does not deserve to be quantized with the phonon contribution.

#### ACKNOWLEDGMENTS

This work was supported by the Deutsche Forschungsgemeinschaft (DFG) through SFB 1143 (Project No. 247310070), through Project No. HE3439/13, and through Grant No. KA 1694/12-1. The work at Peking University was supported by the National Basic Research Program of China (Grants No. 2021YFA1401900 and No. 2018YFA0305602)

TABLE I. Fit parameters from parametrization of  $\kappa_{xy}$  according to Eq. (2).

$T$ (K)	$a_1$ ( $10^{-3} \text{ T}^{-1}$ )	$a_2$ [ $10^{-3} \text{ W (TK m)}^{-1}$ ]
8	-1.716	2.862
9	-2.314	5.304
16	-0.482	1.739
21	-1.751	9.845
26	-2.170	16.096
30	-1.253	10.336
35	-0.592	5.087
37	-0.560	5.089
39	-0.625	5.613
43	-0.458	4.106
48	-0.489	4.444
52	-0.412	3.581
52	-0.434	3.909
60	-0.482	4.263
69	-0.558	4.750
79	-0.474	3.813
89	-0.417	3.126
100	-0.565	4.017
112	-0.625	4.179

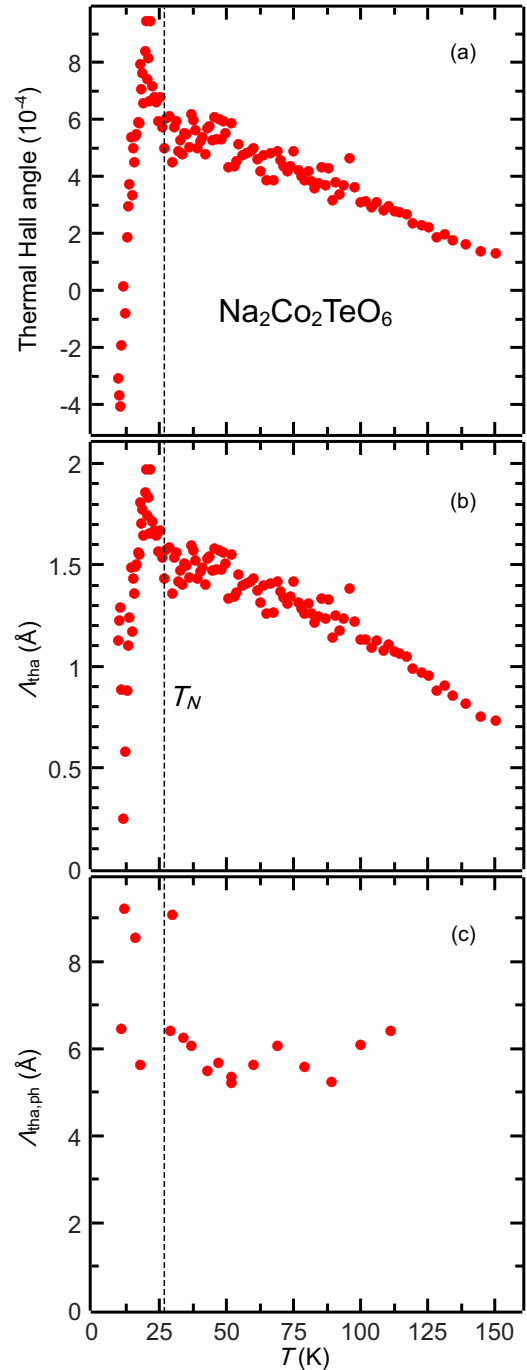


FIG. 12. Temperature dependence of (a) the thermal Hall angle, (b)  $\Lambda_{\text{tha}}$ , and (c)  $\Lambda_{\text{tha,ph}}$  in  $\text{Na}_2\text{Co}_2\text{TeO}_6$ .

and the National Natural Science Foundation of China (Grant No. 12061131004).

#### APPENDIX A: ELECTRON SPIN RESONANCE

The HF-ESR spectrum of  $\text{Na}_2\text{Co}_2\text{TeO}_6$  in the magnetically ordered state for magnetic field applied parallel to the crystal  $c$  axis consists of a single absorption line corresponding to a uniform  $k = 0$  magnon excitation of an antiferromagnetically ordered spin lattice. The resonance field  $H_{\text{res}}$  of this line scales linearly with the excitation frequency  $\nu$  and follows the



relation  $\nu = \Delta + h^{-1}g_c\mu_0\mu_B H$  (Fig. 6). From the slope of this dependence the  $c$  axis component of the  $g$  factor tensor can be determined, amounting to  $g_c = 3.91$ , a value typical for a  $\text{Co}^{2+}$  ion in a distorted octahedral ligand coordination (see, e.g., Refs. [61,62]). Importantly, the data reveal a zero-field excitation gap  $\Delta = 219$  GHz (0.91 meV), which corresponds well to the magnitude of the magnon gap at the  $\Gamma$  point in the 2D Brillouin zone found in a recent inelastic neutron scattering work [49].

As can be seen in Fig. 7, for a given fixed excitation frequency, this  $k = 0$  magnon mode shifts with increasing temperature to higher magnetic fields, obviously due to a softening (decreasing) of the magnon gap  $\Delta$ . By approaching the Néel ordering temperature  $T_N \approx 27$  K this mode substantially broadens and becomes practically unobservable at  $T > T_N$ , possibly due to the thermal population of the excited multiplet states of the  $\text{Co}^{2+}$  ion [61].

## APPENDIX B: ANALYSIS OF $\kappa_{xy}$

The thermal Hall effect data are analyzed according to the empirical equation (2). The explicit field dependence of  $\kappa_{xy}$  is fitted at 8, 9, 16, 21, 37, and 52 K (open symbols in Fig. 8). Error bars in Fig. 5 represent the difference between weighting the data at high and low field, above and below 8 T, respectively.

For temperatures above  $T_N$ , constant temperature cuts of  $\kappa_{xy}(T)$  data (Fig. 9) and  $\kappa_{xx}$  data (Fig. 10) for 0, 6, and 16 T were fitted separately. Error bars for solid symbols in Fig. 5 take into account the spread of  $\kappa_{xy}$  data before averaging by the highest and lowest deviation from the mean value. The temperature dependence of the fit parameters  $a_1$  and  $a_2$  is shown in Fig. 11.

Figure 12 shows the thermal Hall angle  $\kappa_{xy}/\kappa_{xx}$  and the related length scales  $\Lambda_{\text{tha}}$  and  $\Lambda_{\text{tha,ph}}$  for the total thermal Hall signal and its phononic part, respectively.

- 
- [1] A. Kitaev, Anyons in an exactly solved model and beyond, *Ann. Phys. (NY)* **321**, 2 (2006).
- [2] G. Baskaran, S. Mandal, and R. Shankar, Exact results for spin dynamics and fractionalization in the Kitaev model, *Phys. Rev. Lett.* **98**, 247201 (2007).
- [3] J. Knolle, D. L. Kovrizhin, J. T. Chalker, and R. Moessner, Dynamics of a two-dimensional quantum spin liquid: Signatures of emergent Majorana fermions and fluxes, *Phys. Rev. Lett.* **112**, 207203 (2014).
- [4] K. W. Plumb, J. P. Clancy, L. J. Sandilands, V. V. Shankar, Y. F. Hu, K. S. Burch, H.-Y. Kee, and Y.-J. Kim,  $\alpha$ - $\text{RuCl}_3$ : A spin-orbit assisted Mott insulator on a honeycomb lattice, *Phys. Rev. B* **90**, 041112(R) (2014).
- [5] Y. Motome and J. Nasu, Hunting Majorana fermions in Kitaev magnets, *J. Phys. Soc. Jpn.* **89**, 012002 (2020).
- [6] Y. Kasahara, K. Sugii, T. Ohnishi, M. Shimozawa, M. Yamashita, N. Kurita, H. Tanaka, J. Nasu, Y. Motome, T. Shibauchi, and Y. Matsuda, Unusual thermal Hall effect in a Kitaev spin liquid candidate  $\alpha$ - $\text{RuCl}_3$ , *Phys. Rev. Lett.* **120**, 217205 (2018).
- [7] Y. Kasahara, T. Ohnishi, Y. Mizukami, O. Tanaka, S. Ma, K. Sugii, N. Kurita, H. Tanaka, J. Nasu, Y. Motome, T. Shibauchi, and Y. Matsuda, Majorana quantization and half-integer thermal quantum Hall effect in a Kitaev spin liquid, *Nature (London)* **559**, 227 (2018).
- [8] R. Hentrich, M. Roslova, A. Isaeva, T. Doert, W. Brenig, B. Büchner, and C. Hess, Large thermal Hall effect in  $\alpha$ - $\text{RuCl}_3$ : Evidence for heat transport by Kitaev-Heisenberg paramagnons, *Phys. Rev. B* **99**, 085136 (2019).
- [9] M. Yamashita, J. Gouchi, Y. Uwatoko, N. Kurita, and H. Tanaka, Sample dependence of half-integer quantized thermal Hall effect in the Kitaev spin-liquid candidate  $\alpha$ - $\text{RuCl}_3$ , *Phys. Rev. B* **102**, 220404(R) (2020).
- [10] E. Lefrançois, G. Grissonnanche, J. Baglo, P. Lampen-Kelley, J.-Q. Yan, C. Balz, D. Mandrus, S. E. Nagler, S. Kim, Y.-J. Kim, N. Doiron-Leyraud, and L. Taillefer, Evidence of a phonon Hall effect in the Kitaev spin liquid candidate  $\alpha$ - $\text{RuCl}_3$ , *Phys. Rev. X* **12**, 021025 (2022).
- [11] J. A. N. Bruin, R. R. Claus, Y. Matsumoto, N. Kurita, H. Tanaka, and H. Takagi, Robustness of the thermal Hall effect close to half-quantization in  $\alpha$ - $\text{RuCl}_3$ , *Nat. Phys.* **18**, 401 (2022).
- [12] A. U. B. Wolter and C. Hess, Spin liquid evidence at the edge and in bulk, *Nat. Phys.* **18**, 378 (2022).
- [13] P. Czajka, T. Gao, M. Hirschberger, P. Lampen-Kelley, A. Banerjee, N. Quirk, D. G. Mandrus, S. E. Nagler, and N. P. Ong, Planar thermal Hall effect of topological bosons in the Kitaev magnet  $\alpha$ - $\text{RuCl}_3$ , *Nat. Mater.* **22**, 36 (2023).
- [14] H. Liu and G. Khaliullin, Pseudospin exchange interactions in  $d^7$  cobalt compounds: Possible realization of the Kitaev model, *Phys. Rev. B* **97**, 014407 (2018).
- [15] W. Yao and Y. Li, Ferrimagnetism and anisotropic phase tunability by magnetic fields in  $\text{Na}_2\text{Co}_2\text{TeO}_6$ , *Phys. Rev. B* **101**, 085120 (2020).
- [16] R. Sano, Y. Kato, and Y. Motome, Kitaev-Heisenberg Hamiltonian for high-spin  $d^7$  Mott insulators, *Phys. Rev. B* **97**, 014408 (2018).
- [17] E. Lefrançois, M. Songvilay, J. Robert, G. Nataf, E. Jordan, L. Chaix, C. V. Colin, P. Lejay, A. Hadj-Azzem, R. Ballou, and V. Simonet, Magnetic properties of the honeycomb oxide  $\text{Na}_2\text{Co}_2\text{TeO}_6$ , *Phys. Rev. B* **94**, 214416 (2016).
- [18] W. Chen, X. Li, Z. Hu, Z. Hu, L. Yue, R. Sutarto, F. He, K. Iida, K. Kamazawa, W. Yu, X. Lin, and Y. Li, Spin-orbit phase behavior of  $\text{Na}_2\text{Co}_2\text{TeO}_6$  at low temperatures, *Phys. Rev. B* **103**, L180404 (2021).
- [19] W. Yao, Y. Zhao, Y. Qiu, C. Balz, J. R. Stewart, J. W. Lynn, and Y. Li, Magnetic ground state of the Kitaev  $\text{Na}_2\text{Co}_2\text{TeO}_6$  spin liquid candidate, *Phys. Rev. Res.* **5**, L022045 (2023).
- [20] W. G. F. Krüger, W. Chen, X. Jin, Y. Li, and L. Janssen, Triple-q order in  $\text{Na}_2\text{Co}_2\text{TeO}_6$  from proximity to hidden-su(2)-symmetric point, *Phys. Rev. Lett.* **131**, 146702 (2023).
- [21] J. Chaloupka, G. Jackeli, and G. Khaliullin, Kitaev-Heisenberg model on a honeycomb lattice: Possible exotic phases

- in iridium oxides  $A_2\text{IrO}_3$ , *Phys. Rev. Lett.* **105**, 027204 (2010).
- [22] J. Chaloupka, G. Jackeli, and G. Khaliullin, Zigzag magnetic order in the iridium oxide  $\text{Na}_2\text{IrO}_3$ , *Phys. Rev. Lett.* **110**, 097204 (2013).
- [23] X. Hong, M. Gillig, R. Hentrich, W. Yao, V. Kocsis, A. R. Witte, T. Schreiner, D. Baumann, N. Pérez, A. U. B. Wolter, Y. Li, B. Büchner, and C. Hess, Strongly scattered phonon heat transport of the candidate Kitaev material  $\text{Na}_2\text{Co}_2\text{TeO}_6$ , *Phys. Rev. B* **104**, 144426 (2021).
- [24] H. Yang, C. Kim, Y. Choi, J. H. Lee, G. Lin, J. Ma, M. Kratochvílová, P. Proschek, E.-G. Moon, K. H. Lee, Y. S. Oh, and J.-G. Park, Significant thermal Hall effect in the 3d cobalt Kitaev system  $\text{Na}_2\text{Co}_2\text{TeO}_6$ , *Phys. Rev. B* **106**, L081116 (2022).
- [25] N. Li, R. R. Neumann, S. K. Guang, Q. Huang, J. Liu, K. Xia, X. Y. Yue, Y. Sun, Y. Y. Wang, Q. J. Li, Y. Jiang, J. Fang, Z. Jiang, X. Zhao, A. Mook, J. Henk, I. Mertig, H. D. Zhou, and X. F. Sun, Magnon-polaron driven thermal Hall effect in a Heisenberg-Kitaev antiferromagnet, [arXiv:2201.11396](https://arxiv.org/abs/2201.11396).
- [26] G. Xiao, Z. Xia, W. Zhang, X. Yue, S. Huang, X. Zhang, F. Yang, Y. Song, M. Wei, H. Deng, and D. Jiang, Crystal growth and the magnetic properties of  $\text{Na}_2\text{Co}_2\text{TeO}_6$  with quasi-two-dimensional honeycomb lattice, *Cryst. Growth Des.* **19**, 2658 (2019).
- [27] A. Alfonsov, K. Mehlawat, A. Zeugner, A. Isaeva, B. Büchner, and V. Kataev, Magnetic-field tuning of the spin dynamics in the magnetic topological insulators  $(\text{MnBi}_2\text{Te}_4)(\text{Bi}_2\text{Te}_3)_n$ , *Phys. Rev. B* **104**, 195139 (2021).
- [28] C. Golze, A. Alfonsov, R. Klingeler, B. Büchner, V. Kataev, C. Mennerich, H.-H. Klauss, M. Goiran, J.-M. Broto, H. Rakoto, S. Demeshko, G. Leibeling, and F. Meyer, Tuning the magnetic ground state of a tetranuclear nickel(II) molecular complex by high magnetic fields, *Phys. Rev. B* **73**, 224403 (2006).
- [29] C. Wellm, J. Zeisner, A. Alfonsov, A. U. B. Wolter, M. Roslova, A. Isaeva, T. Doert, M. Vojta, B. Büchner, and V. Kataev, Signatures of low-energy fractionalized excitations in  $\alpha\text{-RuCl}_3$  from field-dependent microwave absorption, *Phys. Rev. B* **98**, 184408 (2018).
- [30] Y. F. Yang, G.-M. Zhang, and F. C. Zhang, Universal behavior of the thermal Hall conductivity, *Phys. Rev. Lett.* **124**, 186602 (2020).
- [31] G. Grissonnanche, S. Thériault, A. Gourgout, M.-E. Boulanger, E. Lefrançois, A. Ataei, F. Laliberté, M. Dion, J.-S. Zhou, S. Pyon, T. Takayama, H. Takagi, N. Doiron-Leyraud, and L. Taillefer, Chiral phonons in the pseudogap phase of cuprates, *Nat. Phys.* **16**, 1108 (2020).
- [32] M.-E. Boulanger, G. Grissonnanche, S. Badoux, A. Allaire, E. Lefrançois, A. Legros, A. Gourgout, M. Dion, C. H. Wang, X. H. Chen, R. Liang, W. N. Hardy, D. A. Bonn, and L. Taillefer, Thermal Hall conductivity in the cuprate Mott insulators  $\text{Nd}_2\text{CuO}_4$  and  $\text{Sr}_2\text{CuO}_2\text{Cl}_2$ , *Nat. Commun.* **11**, 5325 (2020).
- [33] L. Chen, M.-E. Boulanger, Z.-C. Wang, F. Tafti, and L. Taillefer, Large phonon thermal Hall conductivity in the antiferromagnetic insulator  $\text{Cu}_3\text{TeO}_6$ , *Proc. Natl. Acad. Sci. USA* **119**, e2208016119 (2022).
- [34] G. Xiao, Z. Xia, Y. Song, and L. Xiao, Magnetic properties and phase diagram of quasi-two-dimensional  $\text{Na}_2\text{Co}_2\text{TeO}_6$  single crystal under high magnetic field, *J. Phys.: Condens. Matter* **34**, 075801 (2022).
- [35] S. Zhang, S. Lee, A. J. Woods, W. K. Peria, S. M. Thomas, R. Movshovich, E. Brosha, Q. Huang, H. Zhou, V. S. Zapf, and M. Lee, Electronic and magnetic phase diagrams of Kitaev quantum spin liquid candidate  $\text{Na}_2\text{Co}_2\text{TeO}_6$ , *Phys. Rev. B* **108**, 064421 (2023).
- [36] G. Grissonnanche, A. Legros, S. Badoux, E. Lefrançois, V. Zlatko, M. Lizaire, F. Laliberté, A. Gourgout, J.-S. Zhou, S. Pyon, T. Takayama, H. Takagi, S. Ono, N. Doiron-Leyraud, and L. Taillefer, Giant thermal Hall conductivity in the pseudogap phase of cuprate superconductors, *Nature (London)* **571**, 376 (2019).
- [37] Y. Hirokane, Y. Nii, Y. Tomioka, and Y. Onose, Phononic thermal Hall effect in diluted terbium oxides, *Phys. Rev. B* **99**, 134419 (2019).
- [38] T. Ideue, T. Kurumaji, S. Ishiwata, and Y. Tokura, Giant thermal Hall effect in multiferroics, *Nat. Mater.* **16**, 797 (2017).
- [39] X. Li, B. Fauqué, Z. Zhu, and K. Behnia, Phonon thermal Hall effect in strontium titanate, *Phys. Rev. Lett.* **124**, 105901 (2020).
- [40] K. Sugii, M. Shimozawa, D. Watanabe, Y. Suzuki, M. Halim, M. Kimata, Y. Matsumoto, S. Nakatsuji, and M. Yamashita, Thermal Hall effect in a phonon-glass  $\text{Ba}_3\text{CuSb}_2\text{O}_9$ , *Phys. Rev. Lett.* **118**, 145902 (2017).
- [41] X. Li, Y. Machida, A. Subedi, Z. Zhu, L. Li, and K. Behnia, The phonon thermal Hall angle in black phosphorus, *Nat. Commun.* **14**, 1027 (2023).
- [42] A. Ataei, G. Grissonnanche, M.-E. Boulanger, L. Chen, E. Lefrançois, V. Brouet, and L. Taillefer, Impurity-induced phonon thermal Hall effect in the antiferromagnetic phase of  $\text{Sr}_2\text{IrO}_4$ , [arXiv:2302.03796](https://arxiv.org/abs/2302.03796).
- [43] We point out that Grissonnanche *et al.* reported a sign change of  $\kappa_{xy}$  in doped and thus electrically conducting cuprates [36], which they explained by two contributions with opposite signs, one electronic (which can be well estimated by the Wiedemann-Franz law) and one of unknown origin, which they later identified as phononic [31]. We also stress that this phononic  $\kappa_{xy}$  itself does not exhibit a sign change.
- [44] C. Strohm, G. L. J. A. Rikken, and P. Wyder, Phenomenological evidence for the phonon Hall effect, *Phys. Rev. Lett.* **95**, 155901 (2005).
- [45] B.-G. Jeon, B. Koteswararao, C. B. Park, G. J. Shu, S. C. Riggs, E. G. Moon, S. B. Chung, F. C. Chou, and K. H. Kim, Giant suppression of phononic heat transport in a quantum magnet  $\text{BiCu}_2\text{PO}_6$ , *Sci. Rep.* **6**, 36970 (2016).
- [46] R. Hentrich, A. U. B. Wolter, X. Zotos, W. Brenig, D. Nowak, A. Isaeva, T. Doert, A. Banerjee, P. Lampen-Kelley, D. G. Mandrus, S. E. Nagler, J. Sears, Y.-J. Kim, B. Büchner, and C. Hess, Unusual phonon heat transport in  $\alpha\text{-RuCl}_3$ : Strong spin-phonon scattering and field-induced spin gap, *Phys. Rev. Lett.* **120**, 117204 (2018).
- [47] R. Hentrich, X. Hong, M. Gillig, F. Cagliaris, M. Čulo, M. Shahrokhvand, U. Zeitler, M. Roslova, A. Isaeva, T. Doert, L. Janssen, M. Vojta, B. Büchner, and C. Hess, High-field thermal transport properties of the Kitaev quantum magnet  $\alpha\text{-RuCl}_3$ : Evidence for low-energy excitations beyond the critical field, *Phys. Rev. B* **102**, 235155 (2020).
- [48] M. Gillig, X. Hong, P. Sakrikar, G. Bastien, A. U. B. Wolter, L. Heinze, S. Nishimoto, B. Büchner, and C. Hess, Thermal transport of the frustrated spin-chain mineral linarite: Magnetic

- heat transport and strong spin-phonon scattering, *Phys. Rev. B* **104**, 235129 (2021).
- [49] W. Yao, K. Iida, K. Kamazawa, and Y. Li, Excitations in the ordered and paramagnetic states of honeycomb magnet  $\text{Na}_2\text{Co}_2\text{TeO}_6$ , *Phys. Rev. Lett.* **129**, 147202 (2022).
- [50] J. Callaway, Low-temperature lattice thermal conductivity, *Phys. Rev.* **122**, 787 (1961).
- [51] G. S. Dixon, Lattice thermal conductivity of antiferromagnetic insulators, *Phys. Rev. B* **21**, 2851 (1980).
- [52]  $\partial\kappa_{xx}(H)/\partial H$  is small because at all considered temperatures  $\kappa_{xx}$  has only small variations (less than 10%) around a central value.
- [53] L. Sheng, D. N. Sheng, and C. S. Ting, Theory of the phonon Hall effect in paramagnetic dielectrics, *Phys. Rev. Lett.* **96**, 155901 (2006).
- [54] T. Qin, J. Zhou, and J. Shi, Berry curvature and the phonon Hall effect, *Phys. Rev. B* **86**, 104305 (2012).
- [55] M. Ye, R. M. Fernandes, and N. B. Perkins, Phonon dynamics in the Kitaev spin liquid, *Phys. Rev. Res.* **2**, 033180 (2020).
- [56] M. Ye, L. Savary, and L. Balents, Phonon Hall viscosity in magnetic insulators, [arXiv:2103.04223](https://arxiv.org/abs/2103.04223).
- [57] B. Flebus and A. H. MacDonald, Charged defects and phonon Hall effects in ionic crystals, *Phys. Rev. B* **105**, L220301 (2022).
- [58] P. A. McClarty, X.-Y. Dong, M. Gohlke, J. G. Rau, F. Pollmann, R. Moessner, and K. Penc, Topological magnons in Kitaev magnets at high fields, *Phys. Rev. B* **98**, 060404(R) (2018).
- [59] J. Nasu, J. Yoshitake, and Y. Motome, Thermal transport in the Kitaev model, *Phys. Rev. Lett.* **119**, 127204 (2017).
- [60] H. Katsura, N. Nagaosa, and P. A. Lee, Theory of the thermal Hall effect in quantum magnets, *Phys. Rev. Lett.* **104**, 066403 (2010).
- [61] C. Wellm, W. Roscher, J. Zeisner, A. Alfonsov, R. Zhong, R. J. Cava, A. Savoyant, R. Hayn, J. van den Brink, B. Büchner, O. Janson, and V. Kataev, Frustration enhanced by Kitaev exchange in a  $\tilde{j}_{\text{eff}} = \frac{1}{2}$  triangular antiferromagnet, *Phys. Rev. B* **104**, L100420 (2021).
- [62] M. Iakovleva, T. Petersen, A. Alfonsov, Y. Skourski, H.-J. Grafe, E. Vavilova, R. Nath, L. Hozoi, and V. Kataev, Static magnetic and ESR spectroscopic properties of the dimer-chain antiferromagnet  $\text{BiCoPO}_5$ , *Phys. Rev. Mater.* **6**, 094413 (2022).